Behavior of a chemically doped graphene junction

Damon B. Farmer,[a] Yu-Ming Lin, Ali Afzali-Ardakani, and Phaedon Avouris
IBM T.J. Watson Research Center, Yorktown Heights, New York 10598, USA

(Received 16 February 2009; accepted 2 May 2009; published online 28 May 2009)

Polyethylene imine and diazonium salts are used as complementary molecular dopants to engineer a doping profile in a graphene transistor. Electronic transport in this device reveals the presence of two distinct resistance maxima, alluding to neutrality point separation and subsequent formation of a spatially abrupt junction. Carrier mobility in this device is not significantly affected by molecular doping or junction formation, and carrier transmission is found to scale inversely with the effective channel length of the device. Chemical dilutions are used to modify the dopant concentration and, in effect, alter the properties of the junction. © *2009 American Institute of Physics*.
[DOI: 10.1063/1.3142865]

Since it was first isolated, graphene has become a material of great scientific and technological interest.[1,2] In the absence of appreciable scattering, charge carriers in graphene exhibit extraordinarily high carrier mobilities. As a result, it is considered to be a promising material for device applications. Of particular interest are doped graphene junctions. As a basic building block, junctions are relevant in a wide variety of electronic systems. Understanding the nature of junctions in graphene is therefore crucial in order to realize more complex graphene-based electronics.

Graphene junctions have already revealed interesting phenomena such as fractional quantum Hall transport and Klein tunneling, and they are predicted to produce lensing effects for coherent electrons.[3–5] Most graphene junctions to date have been fabricated and studied via electrostatic doping.[3,6,7] However, due to fabrication constraints and the unavoidable parasitics associated with electrostatic gating, this doping technique may not be readily scalable to a level of technological significance. We therefore investigate chemical doping[8,9] as a route to junction formation in graphene.

Unlike electrostatic doping, chemical doping is scalable and does not introduce significant parasitic capacitances or resistances to nanoelectronic systems.[10,11] Furthermore, the transition width of a chemically doped junction is, in principle, independent of the gate dielectric thickness, allowing for the possibility of spatially abrupt electronic junctions. We have previously identified polyethylene imine (PEI) (*n*-type) and diazonium salts (*p*-type) as stable molecular dopants of graphene.[12] Here, we use these compounds to demonstrate junction formation in a graphene ribbon.

The fabrication process of the graphene device is schematically illustrated in Fig. 1. The ribbon was obtained by mechanical exfoliation of highly oriented pyrolytic graphite and placed on a 300 nm $SiO_2/p+Si$ substrate.[1] Unlike ribbons studied in previous experiments,[13] the 2.48 μm long (L), 50 nm wide (W) ribbon presented here was naturally formed by the transfer process. This eliminates the need for selective etching that can damage the graphene surface. After source and drain electrodes are patterned (0.5 nm Ti/20 nm Pd/30 nm Au), lithography is used to expose half of the ribbon (region B) to the environment while leaving the other half covered with poly(methyl methacrylate) (PMMA) resist (region A). Region B is then treated with a 1 mM solution of 4-(N-hydroxycarboxamido)phenyldiazonium tetrafluoborate in a 19:1 water/methanol mixture for 24 h. This dilute alcohol solution is chosen to prevent swelling and deadhesion of the PMMA mask. After rinsing with copious amounts of water, room temperature (300 K) atomic layer deposition (ALD) is used to deposit 2 nm of Al_2O_3 onto region B. The functional groups of the diazonium compound serve as nucleation sites for ALD,[14] while the Al_2O_3 layer defines region B as *p*-doped and protects the diazonium molecules from subsequent liquid-chemical treatments. After lift-off of the PMMA, the sample is submersed in a 20 wt % solution of PEI in ethanol for 3 h. This allows ample time for the PEI molecules to adsorb onto region A, thereby defining the *n*-doped region of the device. Excess PEI is rinsed off with ethanol, leaving only a thin layer of the polymer absorbed on the sample surface.[15] After this process is completed, the resulting lengths of the ribbon in regions A and B are found to be 1.36 and 1.12 μm, respectively. Electrical measurements of this backgated device are made using a source-drain bias of 10 mV at pressures between 3×10^{-7} and 3×10^{-9} Torr, depending on the ambient temperature.

Room temperature resistance profiles of the device at different points in the fabrication process are shown in

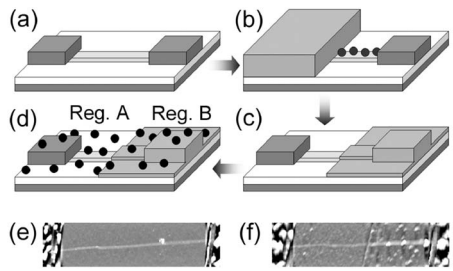

FIG. 1. Schematic of the device fabrication procedure. (a) The as-deposited graphene ribbon. (b) Region A is covered with PMMA and region B is exposed to diazonium salt, where the cation selectively binds to the graphene surface. (c) Region B is coated with 2 nm of Al_2O_3 by ALD, and the PMMA is then removed from region A. (d) A layer of PEI is deposited on the sample surface to complete fabrication. (e) AFM image of the graphene ribbon corresponding to step (a) (L=2.48 μm, W=50 nm). (f) AFM image corresponding to step (d) showing the two well-defined regions (L_A=1.36 μm, L_B=1.12 μm).

[a]Electronic mail: dfarmer@us.ibm.com.

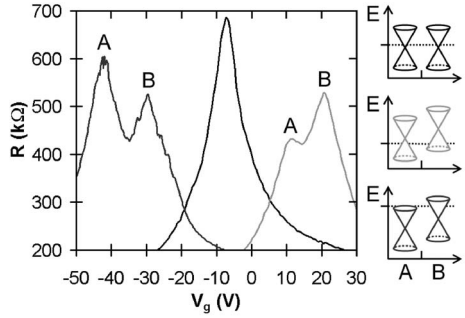

FIG. 2. Resistance profiles at 300 K and corresponding band alignments of the as-deposited device (black), the device after diazonium exposure (light gray), and the completed device after PEI exposure (dark gray). The dotted lines in the schematics mark where $V_g=0$ V, and resistance peaks corresponding to the neutrality points of regions A and B are denoted.

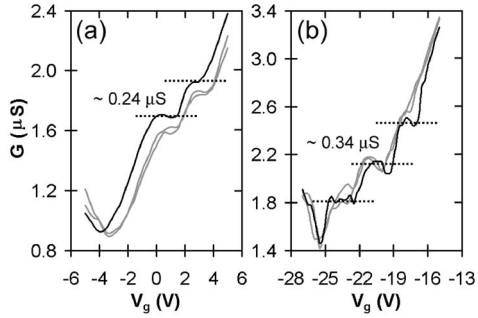

FIG. 3. Electron conductance in the ribbon at different temperatures showing the quantized conductance plateaus before (a) and after (b) junction formation (black: 20 K, gray: 40 and 80 K). The conductance minima of the curves in (b) correspond to the neutrality point of region B.

Fig. 2. The as-deposited device exhibits the standard field-effect characteristics of graphene: a single resistance maxima at the neutrality point voltage (V_{NP}), and a decrease in resistance away from this point, signifying electron ($V_g > V_{\mathrm{NP}}$) and hole ($V_g < V_{\mathrm{NP}}$) conduction. Deviation from this behavior is observed after PMMA masking and diazonium exposure. The nonuniform doping profile established by the masking configuration causes the neutrality points of the two regions to separate (V_{NPA} and V_{NPB}), creating an electronic junction in the ribbon (Fig. 2 schematics). When the magnitude of this separation is sufficiently larger than the thermal energy ($>6k_BT$),[16] the resistance profile reveals these two neutrality points as separate resistance maxima. Estimating the effective capacitance per area (C) of the graphene ribbon to be $C/e=2.83\times10^{11}$ cm^{-2} V^{-1}, and using the expression, $\Delta E=\hbar v_F[\pi(C/e)|V_{\mathrm{NPA}}-V_{\mathrm{NPB}}|]^{1/2}$, the energy separation of the two neutrality points can be determined.[17,18] With a measured value of $|V_{\mathrm{NPA}}-V_{\mathrm{NPB}}|=9.5$ V, the corresponding energy separation between the PMMA and diazonium doped regions is found to be $\Delta E=190$ meV, much larger than $6k_BT$ (150 meV at 300 K). Subsequent PEI deposition results in the completed device with two pronounced resistance peaks, where $|V_{\mathrm{NPA}}-V_{\mathrm{NPB}}|=14$ V and $\Delta E=230$ meV. Ideally, the process illustrated in Fig. 1 should dope the two regions independently of one another. However, it can be seen that both local diazonium exposure and global PEI deposition shifts the neutrality points of both regions. This may be due to the inability of the PMMA and Al_2O_3 masks to completely protect against dopant permeation or is perhaps the result of induced states that allow for electronic penetration into opposing regions.[19] Nevertheless, junction formation of appreciable abruptness is evidenced by the presence of the two resistance maxima.

Figure 3 shows the conductance of electrons in the graphene ribbon before and after junction formation. The corresponding field-effect mobility is calculated using the relation, $\mu=(\Delta G/\Delta V_g)(L/CW)$, where $\Delta G/\Delta V_g$ is the slope of the G-V_g curve away from the neutrality point. This mobility remains the same before and after junction formation ($\mu=210$ cm^2/V s), indicating that dopant-induced scattering is not the dominant scattering mechanism in this device. Due to the small width of the ribbon, the device exhibits conductance quantization that is observable at low temperatures.[16] The height of the conductance step (G_s) is 0.24 μS before and 0.34 μS after junction formation. This increase in G_s indicates an increase in the transmission probability through the ribbon, $t\propto hG_s/4e^2$, which could be due to the decrease in the effective channel length of the device. Since $\Delta E \gg k_BT$, transport through the graphene junction is dominated by the region with the higher resistance, i.e., the region with the fewest number of modes accessible at the Fermi energy. The device can therefore be considered to have an effective channel length approximately equal to the length of the region (A or B) with the higher resistance. Since G_s is measured nearest to the neutrality point of region B, the effective channel length of the device decreases by 45% (1.12 μm/2.48 μm). Therefore, the resulting transmission is expected to increase by 45%, giving rise to an increase of G_s from 0.24 to 0.34 μS, which is consistent with the values of G_s extracted from Fig. 3. The increase in transmission with decreasing effective channel length confirms previous observations made on undoped graphene ribbons of different lengths.[16] Furthermore, the fact that G_s scales inversely with the effective channel length indicates that the junction does not act as a barrier to transport. Since charge carriers in graphene are expected to behave like massless Dirac quasiparticles with $t=1$ through barriers at normal incidence (Klein tunneling),[2,4,20,21] this is not unexpected.

Figure 4 shows the resistance profiles of the junction device at different temperatures and PEI concentrations. The initial state of the device exhibits two resistance maxima that are most apparent at low temperatures, where the peaks are well defined. These peaks are also observable at room temperature but their widths increase due to thermal spreading of the carrier distribution [Fig. 4(a)]. The peaks are separated by a gate voltage interval of $|V_{\mathrm{NPA}}-V_{\mathrm{NPB}}|=14$ V. As calculated above, this corresponds to an energy separation of $\Delta E=230$ meV.

The degree of neutrality point separation can be controlled through modulation of the dopant concentration. More moderate n-doping is achieved by washing the sample in ethanol at 330 K for 8 h, thereby removing some of the adsorbed PEI. Figure 4(b) shows the effect of this ethanol treatment. At low temperatures, the gate voltage separation of the peaks is found to be $|V_{\mathrm{NPA}}-V_{\mathrm{NPB}}|=9$ V, which corresponds to an energy offset of $\Delta E=185$ meV. As expected, PEI reduction causes a decrease in the energy separation of the two neutrality points. Due to thermal spreading and the reduced value of ΔE, the two resistance maxima can no longer be resolved at room temperature. Instead, only a single, broad peak is observed. Further decrease in ΔE is

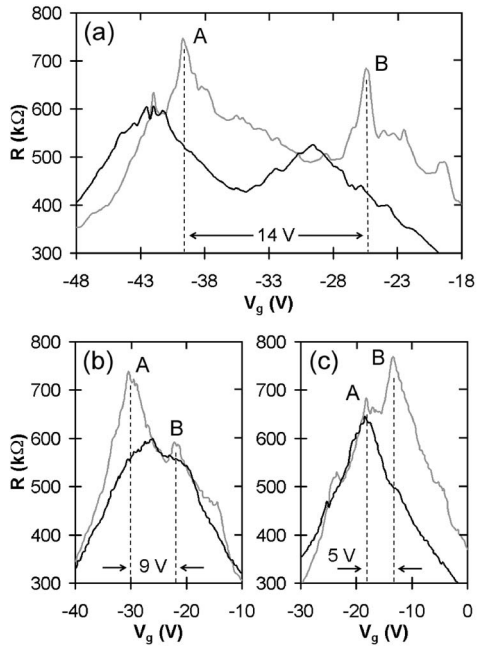

FIG. 4. Transport characteristics of the doped junction at different temperatures and PEI concentrations (black: 300 K, gray: 20 K). (a) Completed device before PEI removal. (b) After an 8 h submersion in ethanol. (c) After a 24 h submersion in ethanol.

accomplished by washing the sample in ethanol for longer periods. Figure 4(c) shows the resistance profile of the device after a 330 K ethanol treatment for 24 h. At this point, PEI is almost completely removed from the device. This is reflected in the reduced value of $|V_{\mathrm{NPA}}-V_{\mathrm{NPB}}|=5$ V. Now, the neutrality points of the two regions are only separated by $\Delta E = 140$ meV. As in the previous case, the two maxima are only observable at low temperatures. However, the single peak at room temperature is comparably sharper because the energy separation of the neutrality points has been reduced. The overall trend of decreasing ΔE with decreasing PEI concentration is unmistakable.

In summary, diazonium salts and PEI have been used to create a stable doping profile in a graphene ribbon. Conductance analysis reveals that the dopants preserve both the mobility of the charge carriers and the transmission of these carriers through the ribbon. The doping profile separates the neutrality point energies of the two doped regions, causing a junction to form at their interface. Modulation of this profile is achieved through chemical dilutions of the dopant concentration. By doing this, a degree of control over the junction properties is attained.

[1] K. S. Novoselov, A. K. Geim, S. V. Morozov, D. Jaing, Y. Zhang, S. V. Dubonos, I. V. Grigorieva, and A. A. Firsov, Science **306**, 666 (2004).
[2] A. K. Geim and K. S. Novoselov, Nature Mater. **6**, 183 (2007).
[3] J. R. Williams, L. DiCarlo, and C. M. Marcus, Science **317**, 638 (2007).
[4] N. Stander, B. Huard, and D. Goldhaber-Gordon, Phys. Rev. Lett. **102**, 026807 (2009).
[5] V. V. Cheianov, V. Fal'ko, and B. L. Altshuler, Science **315**, 1252 (2007).
[6] B. Huard, J. A. Sulpizio, N. Stander, K. Todd, B. Yang, and D. Goldhaber-Gordon, Phys. Rev. Lett. **98**, 236803 (2007).
[7] B. Özyilmaz, P. Jarillo-Herrero, D. Efetov, D. A. Abanin, L. S. Levitov, and P. Kim, Phys. Rev. Lett. **99**, 166804 (2007).
[8] F. Schedin, A. K. Geim, S. V. Morozov, E. W. Hill, P. Blake, M. I. Katsnelson, and K. S. Novoselov, Nature Mater. **6**, 652 (2007).
[9] J.-H. Chen, C. Jang, S. Adam, M. S. Fuhrer, E. D. Williams, and M. Ishigami, Nat. Phys. **4**, 377 (2008).
[10] Y.-M. Lin, J. Appenzeller, J. Knoch, and Ph. Avouris, IEEE Trans. Nanotechnol. **4**, 481 (2005).
[11] Y. Nosho, Y. Ohno, S. Kishimoto, and T. Mizutani, Nanotechnology **18**, 415202 (2007).
[12] D. B. Farmer, R. Golizadeh-Mojarad, V. Perebeinos, Y.-M. Lin, G. S. Tulevski, J. C. Tsang, and Ph. Avouris, Nano Lett. **9**, 388 (2009).
[13] Z. Chen, Y.-M. Lin, M. J. Rooks, and Ph. Avouris, Physica E **40**, 228 (2007).
[14] D. B. Farmer and R. G. Gordon, Electrochem. Solid-State Lett. **8**, G89 (2005).
[15] M. Shim, A. Javey, N. W. S. Kam, and H. Dai, J. Am. Chem. Soc. **123**, 11512 (2001).
[16] Y.-M. Lin, V. Perebeinos, Z. Chen, and Ph. Avouris, Phys. Rev. B **78**, 161409(R) (2008).
[17] J. Yan, Y. Zhang, P. Kim, and A. Pinczuk, Phys. Rev. Lett. **98**, 166802 (2007).
[18] Since the dopants will undoubtedly effect the electric field distribution from the ribbon and the corresponding value of C, the calculated values of ΔE are approximate.
[19] F. Xia, T. Mueller, R. Golizadeh-Mojarad, M. Freitag, Y.-M. Lin, J. C. Tsang, V. Perebeinos, and Ph. Avouris, Nano Lett. **9**, 1039 (2009).
[20] M. I. Katsnelson, K. S. Novoselov, and A. K. Geim, Nat. Phys. **2**, 620 (2006).
[21] A. F. Young and P. Kim, Nat. Phys. **5**, 222 (2009).